SCIENTIFIC REPORTS

OPEN

SUBJECT AREAS:
EMBRYOLOGY
PREDICTIVE MARKERS
INTRAUTERINE GROWTH

Received
12 November 2013

Accepted
19 March 2014

Published
16 April 2014

Correspondence and requests for materials should be addressed to K.M. (miyado-k@ncchd.go.jp) or T.H. (toshiohamatani@z3.keio.jp)

* These authors contributed equally to this work.

Absence of CD9 reduces endometrial VEGF secretion and impairs uterine repair after parturition

Natsuko Kawano[1]*, Kenji Miyado[1], Noriko Yoshii[2]*, Seiya Kanai[1], Hidekazu Saito[3], Mami Miyado[4], Noboru Inagaki[5], Yasushi Odawara[2], Toshio Hamatani[6] & Akihiro Umezawa[1]

[1]Department of Reproductive Biology, National Research Institute for Child Health and Development, 2-10-1 Okura, Setagaya, Tokyo, Japan, [2]Fertility Clinic Tokyo, 3-13-11 Higashi, Shibuya, Tokyo, Japan, [3]Department of Perinatal Medicine and Maternal Care, National Center for Child Health and Development, 2-10-1 Okura, Setagaya, Tokyo, Japan, [4]Department of Molecular Endocrinology, National Research Institute for Child Health and Development, Tokyo, Japan, [5]Saint Women's Clinic, 9-1 Higashitakasagocho, Urawa, Saitama, Japan, [6]Department of Obstetrics and Gynecology, Keio University School of Medicine, 35 Shinanomachi, Shinjuku, Tokyo, Japan.

In mammals, uterine epithelium is remodeled cyclically throughout adult life for pregnancy. Despite the expression of CD9 in the uterine epithelium, its role in maternal reproduction is unclear. Here, we addressed this issue by examining uterine secretions collected from patients undergoing fertility treatment and fertilization-competent *Cd9*$^{-/-}$ mice expressing CD9-GFP in their eggs (*Cd9*$^{-/-}$*TG*). CD9 in uterine secretions was observed as extracellular matrix-like feature, and its amount of the secretions associated with repeated pregnancy failures. We also found that the litter size of *Cd9*$^{-/-}$*TG* female mice was significantly reduced after their first birth. Severely delayed re-epithelialization of the endometrium was then occurred. Concomitantly, vascular endothelial growth factor (VEGF) was remarkably reduced in the uterine secretions of *Cd9*$^{-/-}$*TG* female mice. These results provide the first evidence that CD9-mediated VEGF secretion plays a role in re-epithelialization of the uterus.

In humans, remodeling events that occur naturally in the uterus, namely menstruation and parturition, have features in common with tissue injury and repair in other tissues[1,2]. During such remodeling in the uterus, the human endometrium undergoes the menstrual cycle[1], whereas most other mammals are subjected to the estrous cycle[2]. In humans and mice, the endometrium commonly grows to a thick and blood vessel-rich glandular layer, providing the optimal environment for implantation of blastocysts in the uterine tissue[3]. The endometrium consists of a columnar epithelium and connective tissues that vary in thickness by hormonal control, and undergoes extensive epithelial turnover throughout adult female life[3]. The endometrium also prevents adhesion between the opposing walls of muscular layers in the uterus, termed the myometrium, thereby maintaining the patency of the uterine cavity[3].

In mice, the estrous cycle is divided into two ovarian phases, follicular and luteal phases[2]. The follicular phase is the period of ovarian follicle development consisting of proestrus and estrus stages, whereas the luteal phase is the period of corpus luteum formation and function comprising metestrus and diestrus stages[2]. The uterus is distended during proestrus and estrus stages because of the increase in uterine vascular permeability and accumulation of uterine secretions. This distention decreases in the midestrus stage, and it is no longer observed during the diestrus stage. The four stages of the estrous cycle are easily distinguished by the vaginal smear test[4].

CD9 gene encoding a 24-kDa protein is transcribed in all types of mammalian cells[5]. This protein is localized on the cell membranes and partly on endosomes, and it is expected to be involved in cell-cell adhesion, because CD9 associates with integrin family[5]. CD9 is also known as a motility-related protein 1 (MRP-1), which plays a role in suppressing tumor metastasis[6]. The pregnancy-specific glycoproteins (Psg) are secreted hormones encoded by multiple genes in rodents and primates, and the only Psg receptor identified is CD9[7]. Although Psg proteins are associated predominantly with endothelial cells lining vascular channels in the decidua, maternal CD9 is not essential for successful pregnancy[7]. CD9 belongs to a membrane protein family, collectively termed "tetraspanin", which encompasses 35 members in mammals, such as CD9, CD37, CD53, CD63, CD81, CD82, and CD151[5].

Nano-sized microvesicles, termed exosomes, are released from various cell types and play a role in transferring cellular materials from cell to cell[8]. They contain heat shock proteins, HSP70 and HSP90, present tetraspanins,

CD9, CD81, and CD63, and gangliosides, GM1 and GM3, on their outer membrane[9,10], and often carry ribonucleotides including mRNA and microRNA[11]. In dendritic cells, exosomes are generated from intraluminal endosomal vesicles, which are then released from the cell surface as multivesicular bodies[12].

CD9 plays a crucial role in sperm-egg fusion, and *Cd9*-deficient eggs are unable to fuse with sperm[13–15]. Moreover, CD9-containing exosome-like vesicles, namely egg exosomes, are released from eggs and transferred to the sperm head to facilitate sperm-egg fusion[16].

Some evidence in somatic cells and eggs has indicated the presence of two forms of exosomes, the former with intact lipid bilayers[8] and the latter without typical lipid bilayers[16,17]. In the endometrium, CD9 is predominantly distributed in the lateral membranes of epithelial cells[18]. However, in $Cd9^{-/-}$ female mice, no overt abnormalities have been reported in uterine function for pregnancy. Here, we focus on the role of CD9 in the uterus, more specifically endometrial epithelial cells.

Results

Extracellular presence of CD9 in mouse uterine secretions. In mice, CD9-containing exosomes are present in the extracellular region of eggs[16,17]. Hence, we considered that CD9 might be present extracellularly in the inner cavity of the uterus. Because the inner cavity is filled with uterine secretions during estrus, we first carried out immunostaining for CD9 in the endometrium at the estrus stage in 8–9-week-old C57BL/6N female mice (Fig. 1a). When we used anti-mouse CD9 mAb raised against the extracellular loop of CD9[19]. CD9 was intensely expressed on the epithelial layers, and its intensity in the inner layer was stronger than that in the outer layer. Furthermore, in the outer layer, CD9 was localized at the basolateral region, but not the apical region (Fig. 1b).

Next, we estimated the amount of CD9 in the uterine secretions collected from mice at each stage of the estrus cycle by immunoblotting with anti-mouse CD9 mAb. As depicted in Fig. 1c, CD9 was detected at all four stages and the amount of CD9 in the estrus stage was strikingly higher than that in other stages (Fig. 1d, Supplementary Fig. 1a). Furthermore, to remove blood and epithelial cells, the uterine secretions were centrifuged and then subjected to immunoblotting (Supplementary Fig. 1b). Despite the removal of cells, CD9 was strongly detected in the supernatant (Supplementary Fig. 1c). Moreover, when we carried out immuno-electron microscopic analysis of CD9 in the uterine secretions, the gold particles conjugated to the anti-CD9 mAb reacted with extracellular matrix-like structures (Fig. 1e, g) that were distinct from typical exosomes with lipid bilayers (arrows in Fig. 1f). As depicted in Fig. 1h, these results suggest that extracellular CD9 is present in the uterine cavity and the amount of CD9 increases in a female reproductive cycle-dependent manner.

Correlation between the secreted CD9 and recurrent implantation failure (RIF) in patients. In humans, CD9 is expressed in the endometrial epithelium and localized on the cell membrane[20], but its extracellular presence is unknown. Therefore, we carried out immunoblotting for CD9 in human uterine flushing collected from the uterine cavity of subfertile patients. CD9 was detected in some samples (Fig. 2a, Supplementary Fig. 2a), but the total protein concentration in samples did not correlate with the amount of CD9 (Supplementary Fig. 2b). These results suggest that CD9 is present either in a soluble extracellular form or on exosomes in uterine fluid, and that patients can be divided into CD9-positive and CD9-negative groups. Therefore, we determined whether the absence of CD9 contributed to any clinical features in patients.

We examined the correlation between the presence of CD9 in uterine flushing and RIF. Two patient groups were recruited; those with RIF (37.1 ± 3.2 years old) and a control within 6 months since their first visit at clinics with complaint of infertility (36.4 ± 4.5 years old) (Supplementary Table 1a). The CD9-negative rate in patients with RIF (65.2%, n = 115) was significantly higher than that in the control (44.6%, n = 56) (Fig. 2b, Supplementary Table 1a). When the RIF patients were separated into those with or without a history of dilatation and curettage (D&C), the CD9-negative rate was significantly higher in patients with a history of D&C (78.1%, n = 32) than those without a history of D&C (53.1%, n = 49) (Fig. 2c, Supplementary Table 1b). Furthermore, when the RIF patients were separated into those with thin endometrium at the mid luteal phase (<8.5 mm by transvaginal ultrasound) or those with normal-width endometrium (≥8.5 mm), the CD9-negative rate was significantly higher in the RIF patients with thin endometrium (81.8%, n = 22) than those with normal endometrium (49.3%, n = 69) (Fig. 2d, Supplementary Table 1c). These results suggest that lack of CD9 might be associated with insufficient repair of endometrial injury and consequent thin endometrium. Moreover, we studied if the presence of CD9 in uterine flushing influences on the prognosis of the RIF patients. When the RIF patients were classified into four groups based on the presence of CD9 in uterine flushing and endometrial thickness at the mid luteal phase, the miscarriage rate for the RIF patients with CD9 (−) and thin endometrium was the highest (66.7%, n = 9), compared to those with CD9 (+) and thin endometrium (50.0%, n = 6), those with CD9 (+) and normal endometrium (42.9%, n = 7), and those with CD9 (−) and normal endometrium (15.0%, n = 20) (Fig. 2e, Supplementary Table 1d). As depicted in Fig. 2f, the absence of extracellular CD9 in the uterine cavity might be linked to insufficient repair of endometrial injury, endometrial thinning, and implantation failure.

Delayed repair of $Cd9^{-/-}$ endometrial epithelium. To explore the role of CD9 in the endometrium, we examined $Cd9^{-/-}$ female mice that are severely subfertile because of a strongly reduced ability of egg fusion with sperm. We previously generated fertilization-competent $Cd9^{-/-}$ mice expressing GFP-tagged CD9 (CD9-GFP) only in their eggs ($Cd9^{-/-}TG$)[16]. As depicted in Fig. 3a, after mating $Cd9^{-/-}TG$ female mice with $Cd9^{-/-}$ male mice, we quantitated the resulting litter size. Concomitantly, $Cd9^{+/+}$ female mice were mated with $Cd9^{-/-}$ male mice as a control. In general, the litter size of mice exhibits an age-dependent reduction, but the reduction of the litter size of $Cd9^{-/-}TG$ mice did not depend on their age (Fig. 3b). Therefore, we rearranged the litter size in a new order depending on parturition times (Fig. 3c). Although, the first litter size of $Cd9^{-/-}TG$ mice was comparable to that of $Cd9^{+/+}$ mice (7.2 ± 0.2 vs. 8.1 ± 0.3), the second litter size of $Cd9^{-/-}TG$ mice was significantly reduced compared with that of $Cd9^{+/+}$mice (2.9 ± 0.7 vs. 8.6 ± 0.4; $P < 0.001$). Similarly, the third litter size showed a significant reduction ($Cd9^{-/-}TG$ vs. $Cd9^{+/+}$; 2.8 ± 0.9 vs. 7.8 ± 0.8; $P < 0.001$). Moreover, the fourth litter size was reduced for both $Cd9^{-/-}TG$ and $Cd9^{+/+}$ mice (1.8 ± 0.9 vs. 2.4 ± 1.5). Thus, because the litter size reduction was dependent on parturition in $Cd9^{-/-}TG$ female mice, despite the expression of CD9-GFP in eggs[16], CD9 might also act in the endometrial epithelium.

Therefore, we focused on the process of endometrial repair after the first parturition in $Cd9^{-/-}TG$ female mice. As depicted in Fig. 3a, $Cd9^{-/-}TG$ female mice were mated with $Cd9^{-/-}$ male mice and their uteri were isolated after the first parturition. Concomitantly, $Cd9^{+/+}$ female mice were mated with $Cd9^{-/-}$ male mice. The endometrium of $Cd9^{+/+}$ mice at day 0 after parturition was sectioned and stained with H&E, revealing that the epithelial layer was separated from fetus-attached sites (upper panels in Fig. 3d). In $Cd9^{+/+}$ mice, the endometrium had fragile connective tissues, but was completely sealed by the epithelial layer at day 2 (middle panels in Fig. 3d). On the other hand, in the endometrium of $Cd9^{-/-}TG$ mice at day 5, the stromal layers were exposed on the inner surface of the uterus at the site of fetal attachment and the opposing walls were attached in the myometrium. These features resulted in a partial loss of patency in the uterine cavity (lower panels in Fig. 3d). Further observation at

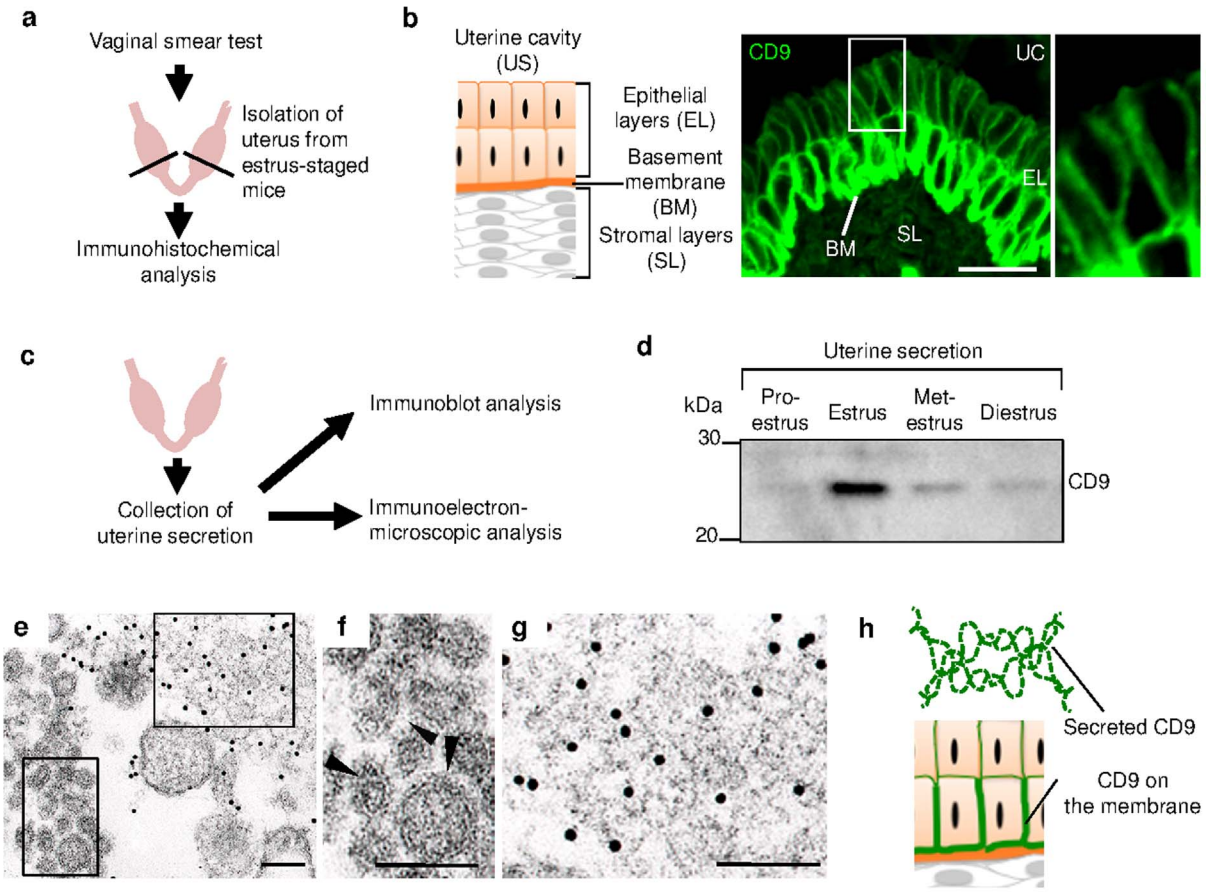

Figure 1 | Detection of extracellular CD9 in uterine secretions. (a), Experimental schematic for immunostaining the endometrial epithelium with an anti-CD9 mAb. After estrus-stage mice were identified by a vaginal smear test, the uterus was isolated and examined by immunohistochemical analysis. (b), As depicted from the left, the endometrium includes epithelial layers (EL), a basement membrane (BM), and stromal layers (SL). The endometrial epithelium was incubated with the anti-CD9 mAb and then an Alexa Fluor 488-labeled secondary antibody. UC, uterine cavity. Arrowheads, CD9-reduced apical regions. Scale bar, 20 μm. (c), Experimental schematic for immunoblotting of uterine secretions at each stage of the estrous cycle, and immuno-electron microscopic analysis of uterine secretions at the estrus stage. (d), Immunoblotting of uterine secretions collected from each stage of the estrous cycle. (e), Immuno-electron microscopic images of uterine secretions at the estrus stage. (f) and (g), Enlarged images of boxes in (e). Scale bars, 100 nm. (h), Schematic of the two types of CD9.

day 21 revealed that the endometrium was completely sealed and the connective tissues were recovered in *Cd9*$^{+/+}$ mice (upper panels in Fig. 3e). However, in *Cd9*$^{-/-}$*TG* mice, the endometrium was not sealed by the epithelial layer, even at the same day, and the uterus had still lost patency (middle and lower panels in Fig. 3e). Based on these results, CD9 deficiency might reduce the motility and proliferation of epithelial cells in the uterus.

In vitro regenerative ability of the Cd9$^{-/-}$TG endometrial epithelium. To examine the regenerative ability of the *Cd9*$^{-/-}$ endometrial epithelium, we carried out a conventional *in vitro* wound healing assay. As depicted in Fig. 3f, after the uterus was isolated from estrus-stage *Cd9*$^{-/-}$*TG* female mice, its inner cavity was treated with collagenase to collect and culture the epithelial cells. Concomitantly, epithelial cells were isolated from *Cd9*$^{+/+}$ female mice for culture. In wound healing assays from 0 to 17.5 hours, the wounds were significantly wide at 3.5 and 17.5 hours in cultures of *Cd9*$^{-/-}$*TG* mouse epithelial cells compared with those in cultures of *Cd9*$^{+/+}$ mouse epithelial cells (3.5 h: 0.82 ± 0.04 vs. 0.60 ± 0.01, $P < 0.007$; 17.5 h: 0.46 ± 0.05 vs. 0.00 ± 0.00, $P < 0.001$; the wound width at 0 h was assigned a relative value of 1) (Fig. 3g, h). This result suggests that the regenerative ability of *Cd9*$^{-/-}$ endometrial epithelial cells is low compared with that of *Cd9*$^{+/+}$ cells.

Cell adhesion-related proteins in the Cd9$^{-/-}$TG endometrium. Repair of the endometrial epithelium is regulated by various physiological events such as cell-cell adhesion, cell motility, and cell growth[1]. In cell-cell adhesion, cadherins and integrins are known to be involved in endometrial repair[21]. In addition, CD98 is a multifunctional type II glycoprotein involved in amino acid transport, cell fusion, and integrin-dependent cell spreading[22]. CD98 is thought to function as a receptivity determinant, because its expression is undetectable outside of the implantation window[20]. According to these previous studies, we examined the localization of integrin α6 and β1, and CD98 in the *Cd9*$^{-/-}$ *TG* endometrium. Integrin α6 was normally localized at the basolateral membrane in *Cd9*$^{-/-}$*TG* mice similar to that in *Cd9*$^{+/+}$ mice (upper panels in Supplementary Fig. 3). Basolateral and apical membrane localization of integrin β1 was also unchanged in the *Cd9*$^{-/-}$ endometrial epithelium (lower panels in Supplementary Fig. 3). Furthermore, the basolateral localization of E-cadherin was indistinguishable between *Cd9*$^{-/-}$*TG* and *Cd9*$^{+/+}$ mice (upper panels in Supplementary Fig. 4). In addition, localization of CD98 at the apical and basal membrane was unaltered in *Cd9*$^{-/-}$*TG* mice compared with that in *Cd9*$^{+/+}$ mice (lower panels in Supplementary Fig. 4). Thus, these cell adhesion-related proteins act normally in the *Cd9*$^{-/-}$*TG* endometrial epithelium.

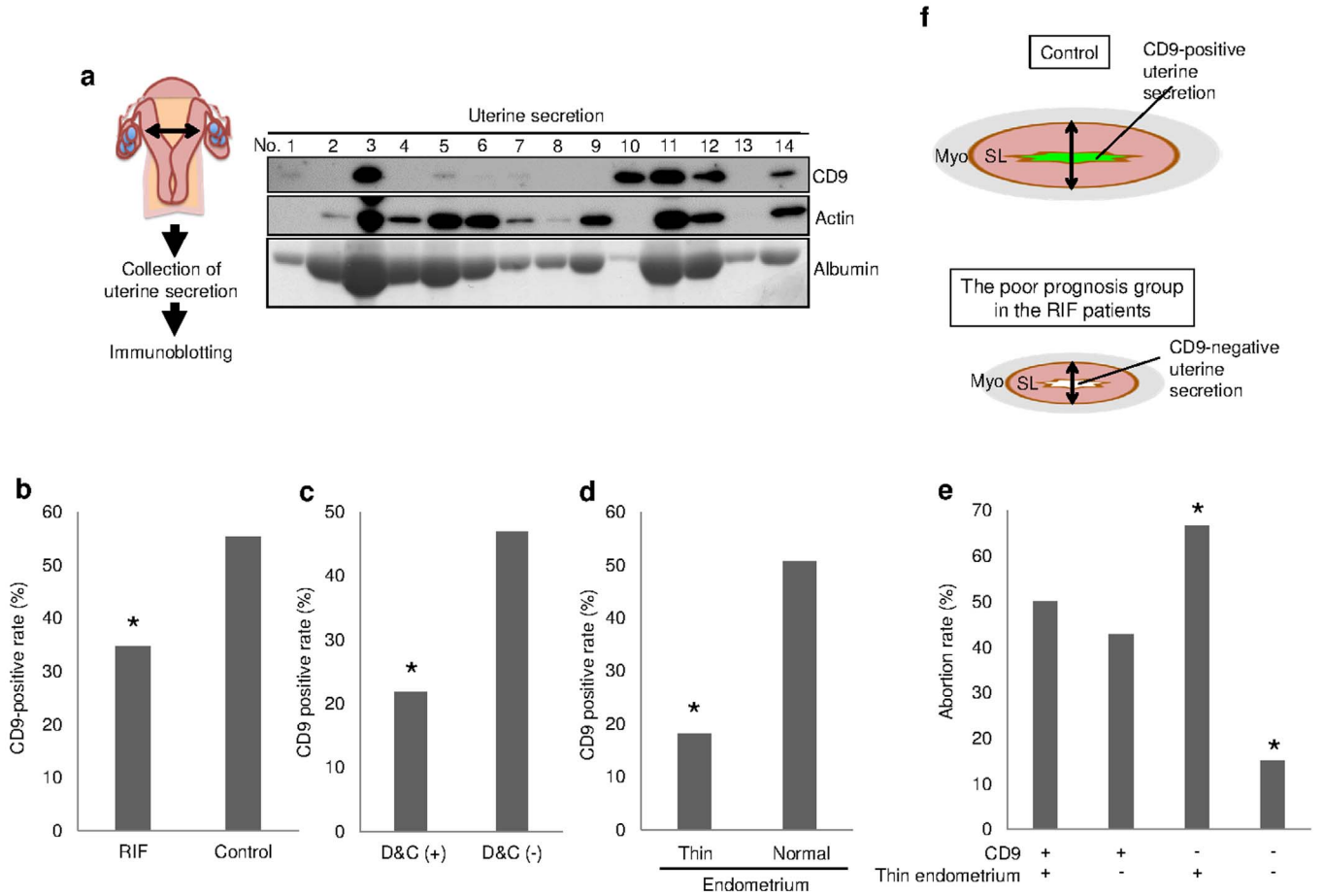

Figure 2 | Immunoblotting of uterine secretions collected from patients undergoing fertility treatment. (a), Uterine secretions were collected from the uterine cavity and examined by immunoblotting. Human samples were immunoblotted with anti-CD9 and anti-β-actin-mAbs, and stained with Coomassie brilliant blue for detection of albumin. The number of samples is shown. (b), The presence of CD9 in uterine flushing in recurrent implantation failure (RIF) patients (n = 115) and the control patients (n = 56). A significant difference among the mean values with asterisk was observed ($P < 0.05$). (c), The association of the CD9 presence with a history of dilation and curettage (D&C) in the RIF patients (D&C[+], n = 22; D&C[−], n = 49). A significant difference among the mean values with asterisk was observed ($P < 0.05$). (d), The association of the CD9 presence with endometrial thickness in the RIF patients. When endometrium width measured by vaginal ultrasound was less than 8.5 mm at the mid luteal phase, the endometrium was categorized as thin endometrium (n = 22). When the width was 8.5 mm or more than that, the endometrium was categorized normal-width endometrium (n = 69). A significant difference among the mean values with asterisk was observed ($P < 0.05$). (e), The association of the CD9 presence with prognosis (miscarriage rates) in the RIF patients. The RIF patients were classified into four groups: those with CD9 (+) and normal endometrium (n = 7), those with CD9 (+) and thin endometrium (n = 6), those with CD9 (−) and normal endometrium (n = 20), and those with CD9 (−) and thin endometrium (n = 9). A significant difference among the mean values that have different superscripts was observed ($P < 0.05$). The endometrial thickness was measured by ultrasound and magnetic resonance imaging at the site indicated with the line in (a), and double-headed arrows in (f). (f), Schematic explanation of a hypothetical relationship between the absence of CD9 and endometrial thinning in the RIF patients.

Cytokines in uterine secretions. In general, tissue remodeling is tightly controlled in a spatiotemporal manner by a complex network of regulators including cytokines[23]. Because immune cells are recruited into the endometrium during repair[24], there is the possibility that CD9 deficiency may directly or indirectly affect the amounts of cytokines in uterine secretions.

Therefore, we first estimated the amounts of cytokines of interest in the uterine secretions using a multiplex suspension array (Supplementary Fig. 5a). The interleukin (IL)-1 family is known to initiate inflammatory responses and play an important role in the physiology of the human endometrium[25]. To explore the possible involvement of IL-1 in uterine repair, we compared the amounts of IL-1α and IL-1β between *Cd9*$^{-/-}$*TG* and *Cd9*$^{+/+}$ mice. The amount of IL-1α in *Cd9*$^{-/-}$ *TG* mice was slightly decreased compared with that in *Cd9*$^{+/+}$ mice (65.2 ± 5.0 vs. 90.1 ± 11.7 pg/ml; P = 0.017) (Supplementary Fig. 5b). On the other hand, there was no difference in the amount of IL-1β between *Cd9*$^{-/-}$*TG* and *Cd9*$^{+/+}$ mice (38.4 ± 2.6 and 46.3 ± 4.9 pg/ml) (Supplementary Fig. 5b). These results imply a reduction in the amount of IL-1α, but sustained total activity of the IL-1 family.

IL-2 is necessary for growth, proliferation, and differentiation of T cells. Makkar et al.[26] reported that a low pregnancy rate is associated with increased expression of IL-2 in the endometrium. To evaluate the involvement of the IL-2 family in endometrial regeneration, we estimated the amounts of this family of cytokines, namely IL-2, IL-7, IL-9, and IL-15. The results show that the amounts of these cytokines in *Cd9*$^{-/-}$ *TG* mice were comparable to those in *Cd9*$^{+/+}$ mice (IL-2: 9.0 ± 1.3 and 8.6 ± 1.0 pg/ml; IL-7: 4.4 ± 0.3 and 4.9 ± 0.5 pg/ml; IL-15: 20.2 ± 2.8 and 21.7 ± 1.5 pg/ml) (Supplementary Fig. 5c). On the other hand, the amount of IL-9 was slightly reduced in *Cd9*$^{-/-}$*TG* mice compared with that in *Cd9*$^{+/+}$ mice (202.7 ± 8.4 vs. 269.2 ± 23.5 pg/ml; P = 0.031) (Supplementary Fig. 5c). Therefore, the amounts of IL-2, IL-7, IL-9, and IL-15 are maintained in the endometrium.

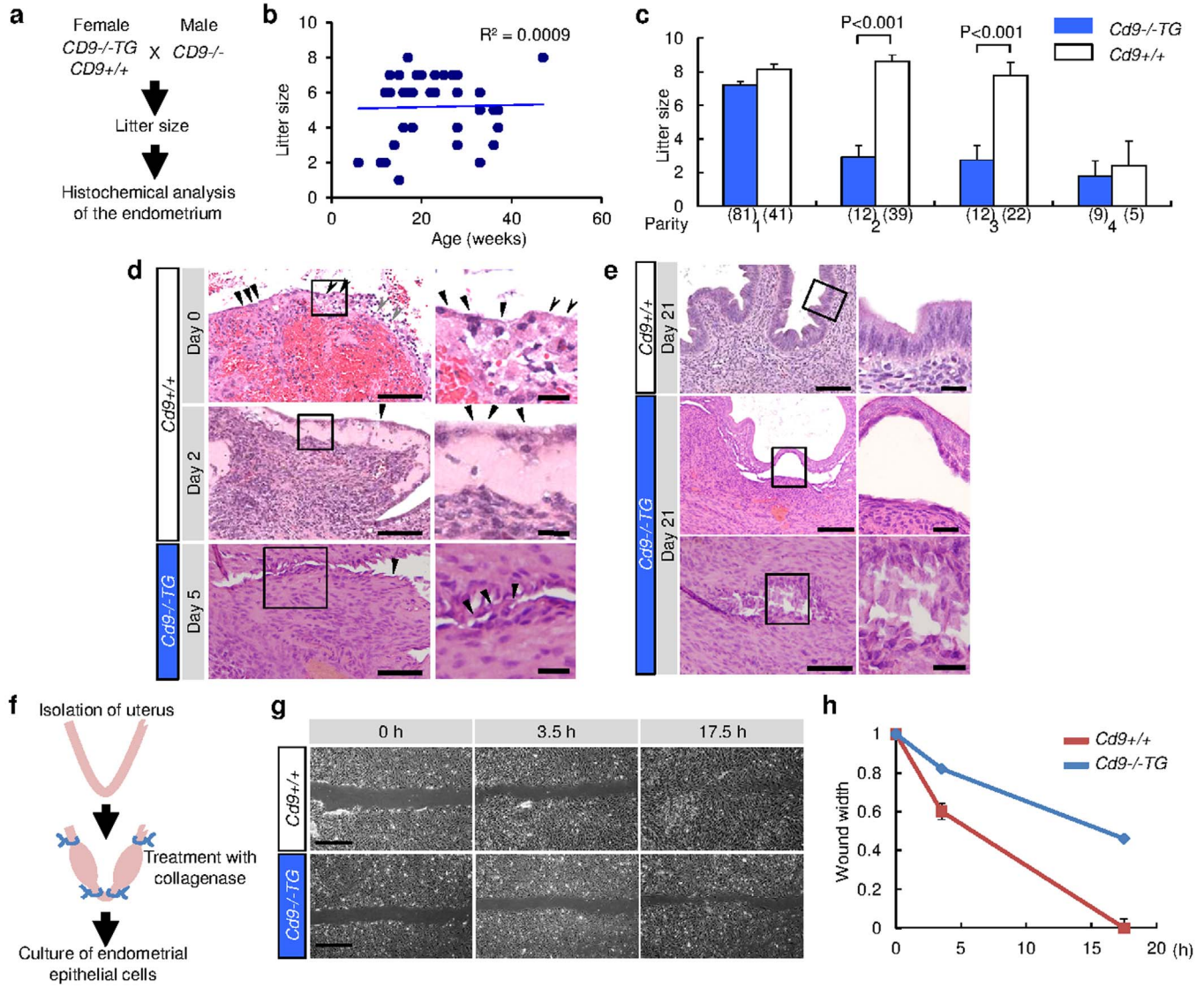

Figure 3 | Reduction of endometrial repair in *Cd9*$^{-/-}$*TG* mice. (a), Experimental schematic for examining the litter size of *Cd9*$^{-/-}$*TG* female mice. (b), Age-independent reduction of the litter size of *Cd9*$^{-/-}$*TG* mice. (c), Reduction of the litter size dependent on parturition in *Cd9*$^{-/-}$*TG* mice. Parenthesis indicates the number of examined mice. Values are the mean ± SEM. (d) and (e), Histochemical analysis of endometrial repair in *Cd9*$^{-/-}$*TG* and *Cd9*$^{+/+}$ mice after parturition (the day of parturition = day 0). (f), Experimental schematic for *in vitro* wound healing assays of the endometrial epithelium of *Cd9*$^{-/-}$*TG* mice. After the uterus was isolated from *Cd9*$^{-/-}$*TG* mice at the estrus stage, collagenase was injected to the intrauterine cavity to collect the epithelial cells. (g), Wounded epithelial cells after scratching the monolayer with a pipette tip. Scale bars, 150 μm. (h), Graph of the wound width of wounded epithelial cells. Values are the mean ± SEM.

IL-3 stimulates the differentiation of hematopoietic stem cells into myeloid and lymphoid progenitor cells, and functions in implantation[27]. Macrophage colony-stimulating factor (M-CSF) is involved in the proliferation, differentiation, and survival of monocytes, macrophages, and bone marrow progenitor cells, and a low serum level of M-CSF is associated with unexplained abortion[28]. In the present study, the amounts of IL-3 and M-CSF in the uterine secretions of *Cd9*$^{-/-}$*TG* mice were comparable to those in *Cd9*$^{+/+}$ mice (IL-3: 3.2 ± 0.1 and 3.1 ± 0.1 pg/ml; M-CSF: 10.8 ± 0.9 and 9.1 ± 0.8 pg/ml) (Supplementary Fig. 5d, e).

Interferon-γ (IFN-γ) is involved in the initiation of uterine vascular modification and maturation of uterine natural killer cells[29]. IL-10 has pleiotropic effects in immunoregulation and inflammation, and inhibits the synthesis of pro-inflammatory cytokines such as IFN-γ, IL-2, and IL-3[30]. In this study, the amounts of IFN-γ and IL-10 in *Cd9*$^{-/-}$*TG* mice were comparable to those in *Cd9*$^{+/+}$ mice (IFN-γ: 6.0 ± 2.7 and 4.6 ± 0.7 pg/ml; IL-10: 55.8 ± 36.3 and 16.4 ± 1.5 pg/ml) (Supplementary Fig. 5f).

IL-12 stimulates the production of IFN-γ in T and natural killer cells[31]. The amount of IL-12 in *Cd9*$^{-/-}$*TG* mice was significantly reduced compared with that in *Cd9*$^{+/+}$ mice (20.9 ± 1.7 vs. 31.4 ± 2.4 pg/ml; $P < 0.001$) (Supplementary Fig. 5g).

Neutrophils are present in large numbers and play an important role during endometrial repair[32]. Granulocyte colony-stimulating factor (G-CSF) stimulates the survival, proliferation, and differentiation of neutrophil precursors and mature neutrophils[33]. The amount of G-CSF was reduced in *Cd9*$^{-/-}$*TG* mice compared with that in *Cd9*$^{+/+}$ mice (761.3 ± 88.6 vs. 4610.4 ± 1955.3 pg/ml; $P = 0.025$) (Supplementary Fig. 5h). However, the number of uterine neutrophils in HE sections was comparable between *Cd9*$^{-/-}$*TG* and *Cd9*$^{+/+}$ mice.

Collectively, these results suggest that the immune system is maintained in the intrauterine cavity of *Cd9*$^{-/-}$*TG* mice, but there might be an impairment of the function of neutrophils.

Chemokines in uterine secretions. C-C motif chemokine-ligand 4 (CCL4) is released from neutrophils[34]. C-X-C motif chemokine

ligand 5 (CXCL5) is a strong chemoattractant for neutrophils[34]. To explore the involvement of these chemokines in the retarded repair of the endometrial epithelium in *Cd9*$^{-/-}$*TG* mice, we examined their amounts in uterine secretions using multiplex suspension arrays as depicted in Supplementary Fig. 5a. As a result, the levels of both chemokines was reduced in uterine secretions of *Cd9*$^{-/-}$*TG* mice (*Cd9*$^{-/-}$*TG* vs. *Cd9*$^{+/+}$; CCL4: 31.3 ± 4.6 vs. 45.1 ± 2.4 pg/ml, $P < 0.001$; CXCL5: 54.3 ± 4.4 vs. 96.0 ± 9.0 pg/ml, $P < 0.001$) (Supplementary Fig. 6a). This result reinforced the idea that neutrophils might be involved in the retarded endometrial repair in *Cd9*$^{-/-}$*TG* mice.

We further quantified the amounts of the following four chemokines in uterine secretions. CCL11, (also called eotaxin), CCL3, (also called macrophage inflammatory protein-1α), and CXCL1 (also called keratinocyte-derived chemokine) are involved in neutrophil recruitment[35]. CCL2, also called monocyte chemotactic protein-1, acts in neutrophil migration[35]. Unexpectedly, the amounts of these chemokines in the uterine secretions of *Cd9*$^{-/-}$*TG* mice were comparable to those of *Cd9*$^{+/+}$ mice (CCL11: 493.4 ± 130.0 vs. 554.9 ± 99.5 pg/ml; CCL3: 65.2 ± 16.4 vs. 44.4 ± 1.7 pg/ml; CXCL1: 23.4 ± 1.1 vs. 23.8 ± 1.5 pg/ml; CCL2: 16.0 ± 1.3 vs. 14.1 ± 2.6 pg/ml) (Supplementary Fig. 6b). These results indicate that neutrophil recruitment is maintained in the uterine secretions of the *Cd9*$^{-/-}$TG mice. Therefore, the immune system functions normally in the uterine secretions of *Cd9*$^{-/-}$*TG* mice.

VEGF and matrix metalloproteinases in uterine secretions of Cd9$^{-/-}$TG mice. VEGF, also called VEGF-A, is a well-known angiogenic factor that is essential for embryonic vasculogenesis and postnatal angiogenesis[36]. Considerable evidence have shown that VEGF also has non-angiogenic functions such as anti-apoptosis and vascular remodeling[37]. To explore the possible involvement of VEGF in uterine repair, we estimated the quantity of VEGF at the estrus stage in uterine secretions of *Cd9*$^{-/-}$TG mice using multiplex suspension arrays as explained in Supplementary Fig. 5a. The results show that the quantity of VEGF was significantly reduced in uterine secretions of *Cd9*$^{-/-}$*TG* mice compared with that in *Cd9*$^{+/+}$ mice (5.4 ± 0.5 vs. 16.6 ± 3.6 pg/ml; $P < 0.001$) (Fig. 4a). To confirm this result, we carried out immunoblotting for VEGF in the uterine secretions of *Cd9*$^{-/-}$*TG* and *Cd9*$^{+/+}$ mice. We detected VEGF in uterine secretions of *Cd9*$^{+/+}$ mice, but not in those of *Cd9*$^{-/-}$*TG* mice (Fig. 4b Supplementary Fig. 7). Three different sized-bands were detected in the uterine secretions of *Cd9*$^{+/+}$ mice. Because VEGF proteins preferentially form homodimers, these were predicted to be the monomer, dimer, and tetramer forms of VEGF as 21, 42, and 84 kDa, respectively, as described previously[38] (Fig. 4b, Supplementary Fig. 7). Matrix metalloproteinases (MMPs) play a role in endometrial repair, especially MMP2, MMP3, MMP7, and MMP11[1]. Tissue inhibitors of MMPs (TIMPs) are also involved in endometrial repair[1], indicating the importance of balanced activities of MMPs and TIMPs. Therefore, we carried out immunoblotting for MMP2, MMP3, MMP7, MMP11, and TIMP1 (Fig. 4b). The levels of MMP2, MMP7, and MMP11 in the uterine secretions of *Cd9*$^{-/-}$*TG* mice were comparable to those of *Cd9*$^{+/+}$ mice. On the other hand, the level of MMP3 was increased in *Cd9*$^{-/-}$*TG* mice compared with that in *Cd9*$^{+/+}$ mice. Furthermore, TIMP1 was detected in uterine cavity of *Cd9*$^{-/-}$*TG* mice, although its expression level was approximately half of that of *Cd9*$^{+/+}$ mice. Because TIMP1-heterozygotes female mice did not show severe phenotypes during fertilization and implantation[39], we considered that the reduced amount of TIMP1 would not affect fertility of *Cd9*$^{-/-}$*TG* mice. These results indicated that the levels of MMPs and TIMP1 in the uterine secretions were different between *Cd9*$^{-/-}$*TG* and *Cd9*$^{+/+}$ mice, but the total MMP activity was balanced in the uterine secretions of *Cd9*$^{-/-}$*TG* mice.

To further examine VEGF expression in the endometrial epithelium of *Cd9*$^{-/-}$*TG* and *Cd9*$^{+/+}$ mice, we carried out immunohistochemical analysis. As shown in Fig. 4c, the uteri of estrus-stage mice were double immunostained for VEGF and CD9, and counterstained with DAPI. The endometrial epithelial cells showed strong expression of VEGF compared with that in the stromal cells of both *Cd9*$^{-/-}$*TG* and *Cd9*$^{+/+}$ mice (Fig. 4c). In contrast, VEGF was present in the intrauterine cavity of *Cd9*$^{+/+}$ mice, but not in that of *Cd9*$^{-/-}$*TG* mice (arrows in Fig. 4c). From the immunohistochemistry, the uterine epithelium displayed elevated expression of VEGF receptor1, Flt-1, but not VEGF receptor2, Flk-1 (Supplementary Fig. 8a). Moreover, as the result from the immunoprecipitation with anti-CD9 antibody followed by blotting with anti-VEGF, the direct interaction between CD9 and VEGF was observed in the uterine fluid collected from *Cd9*$^{+/+}$ mice (Supplementary Fig. 8b). These results suggested that VEGF may be secreted from the endometrial epithelium in a CD9-dependent manner.

VEGF secretion and microvilli extension. To examine the morphological features affecting VEGF secretion, the endometrial epithelium of *Cd9*$^{-/-}$*TG* and *Cd9*$^{+/+}$ mice was examined by electron microscopy. Uteri were isolated from mice staged at estrus or metestrus. In *Cd9*$^{+/+}$ mice at the estrus stage, microvilli were formed on the apical membrane of the endometrial epithelium (hollow arrowheads in upper left panel of Fig. 4d). Similarly, microvilli were formed in the endometrial epithelium of *Cd9*$^{-/-}$*TG* mice, but their length was significantly shorter (arrowheads in lower left panel of Fig. 4d and left graph in Fig. 4e). On the other hand, at the metestrus stage, the short microvilli were present in the endometrial epithelium of both *Cd9*$^{-/-}$*TG* and *Cd9*$^{+/+}$ mice (Supplementary Fig. 9 and right graph in Fig. 4e). In differentiated Caco-2 cells, microvilli are thought to effectively increase the surface area of the cells and are useful for secretion of extracellular vesicles[40]. Because the length of microvilli was significantly shorter at the estrus stage in *Cd9*$^{-/-}$*TG* mice compared with that in *Cd9*$^{+/+}$ mice, we considered that the ability for secretion would be strikingly reduced in the endometrial epithelium of *Cd9*$^{-/-}$*TG* mice. Actually, the uterine cavity of *Cd9*$^{-/-}$*TG* mice was extremely narrow at the estrus stage compared with that of *Cd9*$^{+/+}$ mice (Supplementary Fig. 10), and it was difficult to collect a certain amount of uterine fluid from *Cd9*$^{-/-}$*TG* mice.

Intrauterine treatment of Cd9$^{-/-}$TG endometrial epithelium with VEGF. To explore the contribution of VEGF to the delay of endometrial repair in *Cd9*$^{-/-}$*TG* mice, we injected VEGF into the uterine cavity of *Cd9*$^{-/-}$*TG* mice. As depicted in Fig. 5a, at 1 week after parturition, the VEGF-linked microparticles were injected into the upper region of the left uteri and BSA-linked one as a control were injected into right uteri from the ventral view. The blue microparticles were retained in the uterine cavity even at 1 week after injection (Fig. 5b). To investigate the effects of VEGF treatment, the uteri were sectioned and stained with H&E. In VEGF-treated uteri, the endometrium was fully re-epithelialised (hollow arrowheads in left panels of Fig. 5c). On the other hand, in BSA-treated uteri, the epithelial layers remained limited and the stromal layers were exposed on the endometrium, and the debris including microparticles, decidualised tissues and immune cells was attached to the stromal layers without the epithelium (right panels of Fig. 5c). We counted the number of re-epithelialized regions where fetus had been implanted, and found the re-epithelialization in most VEGF-treated sites, but not in BSA-treated sites (67.5% for VEGF, $n = 8$; 0% for BSA, $n = 13$) (Fig. 5d). In addition, we measured the endometrial thickness and found that the thickness was significantly reduced in *Cd9*$^{-/-}$*TG* mice compared with that in *Cd9*$^{+/+}$ mice (174.5 ± 13.8 μm for VEGF, $n = 15$; 108.0 ± 15.2 μm for BSA, $n = 17$; $P = 0.003$) (Fig. 5e). As depicted in Fig. 5f, our results collectively suggest that the reduction of re-epithelialization in the endometrium of *Cd9*$^{-/-}$*TG* mice is reversed by VEGF treatment, thereby thickening the endometrium. Thus, we propose a novel mechanism

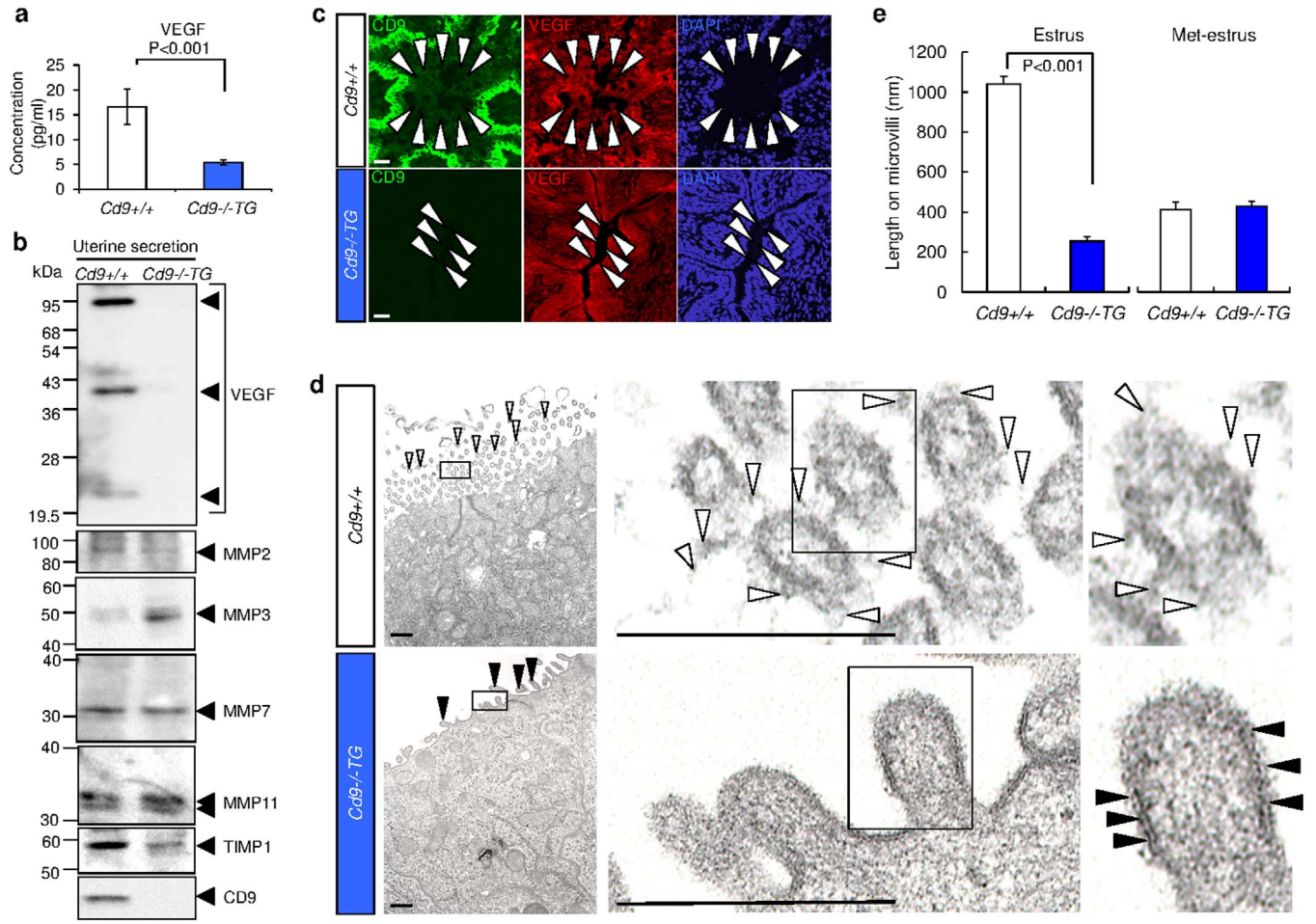

Figure 4 | Decrease of VEGF in uterine secretions of *Cd9*$^{-/-}$*TG* mice. (a), Comparison of the amount of VEGF in uterine secretions of *Cd9*$^{-/-}$*TG* mice at the estrus stage using a multiplex suspension array. (b), Immunoblotting of uterine secretions at the estrus stage in *Cd9*$^{-/-}$*TG* and *Cd9*$^{+/+}$ mice. (c), Immunohistochemical observation of the endometrial epithelium in *Cd9*$^{-/-}$*TG* and *Cd9*$^{+/+}$ mice. White arrowheads indicate the uterine cavity. Scale bars, 20 μm. (d), Electron microscopic images of endometrial epithelial cells in *Cd9*$^{-/-}$*TG* and *Cd9*$^{+/+}$ mice. Left panels, endometrial epithelial cells of *Cd9*$^{-/-}$*TG* and *Cd9*$^{+/+}$ mice at the estrus stage. Middle panels, enlarged images of the boxes in the left panels. Right panels, enlarged images of the boxes in the middle images. Hollow arrowheads indicate the secreted materials in *Cd9*$^{-/-}$*TG* mice. Arrowheads indicate the outer membrane consisting of lipid bilayers in *Cd9*$^{+/+}$ mice. Scale bars, 500 nm. (e), Length of microvilli. Left graph, endometrial epithelial cells at the estrus stage. Right graph, endometrial epithelial cells at the metestrus stage. Values are the mean ± SEM.

of endometrial repair, in which CD9 promotes secretion of VEGF from endometrial epithelial cells and aids the retention of VEGF on the uterine surface (Fig. 5f).

Discussion

The endometrial epithelium undergoes cyclic repair throughout the female reproductive life, but it also undergoes extensive repair because of tissue destruction caused by parturition, both of which are essential for maintenance of mammalian uterine function for pregnancy[2]. Endometrial epithelialization also prevents pathological adhesion between the opposing walls of the endometrium to eventually maintain the space in the uterine cavity required for embryo implantation and subsequent growth[2]. However, there is limited understanding of the mechanism of endometrial repair. Using VEGF blockade, Fan et al.[41] demonstrated that VEGF plays a critical role in early angiogenesis during postmenstrual endometrial repair in both mice and primates. They observed dramatic inhibition of re-epithelialization after VEGF blockade during endometrial repair[41]. The present study provides the first evidence for CD9-mediated VEGF secretion that contributes to endometrial repair (Fig. 5g).

As shown in Fig. 1 and Supplementary Fig. 1, the CD9-containing structure collected from the uterine cavity had no detectable plasma membrane, which was similar to the structure of egg exosomes[16]. Recently, Ng et al.[42] reported that endometrial exosomes including CD9 were observed in the uterine cavity of women. They demonstrated that exosomes of the size of 50–100 nm are present and contain specific miRNAs. These data support our findings that mouse uterine fluid at estrous contains exosome-like particles that are positive for the tetraspanin CD9. In other tissues, CD9 is also detected in extracellular fluid, cerebrospinal fluid from children with acute lymphoblastic leukemia43. Although CD9 is beginning to be recognized as an exosome marker[8,44], the change of the CD9-localization from membrane into the extracellular milieu is largely uncertain. In malignant or transformed cells, it has been known that the release of glycoproteins from the cell membrane is an active process named shedding[43,45,46]. Because CD9 has a potential N-glycosylation site in its extracellular loop, it has been suggested that CD9 is released from cells as one of these glycoproteins[43]. To our knowledge, however, there is no evidence that CD9 is actually glycosylated, and the molecular size of CD9 detected in the uterine was definitely consistent with its non-glycosylated size (24 kDa) (Figs. 1, 2 and 4). In previous paper, we observed the microvilli and the exosomes including CD9 in perivitelline space between egg plasma membrane and zona-pellucida in matured eggs of *Cd9*$^{+/+}$ mice, but not in that of

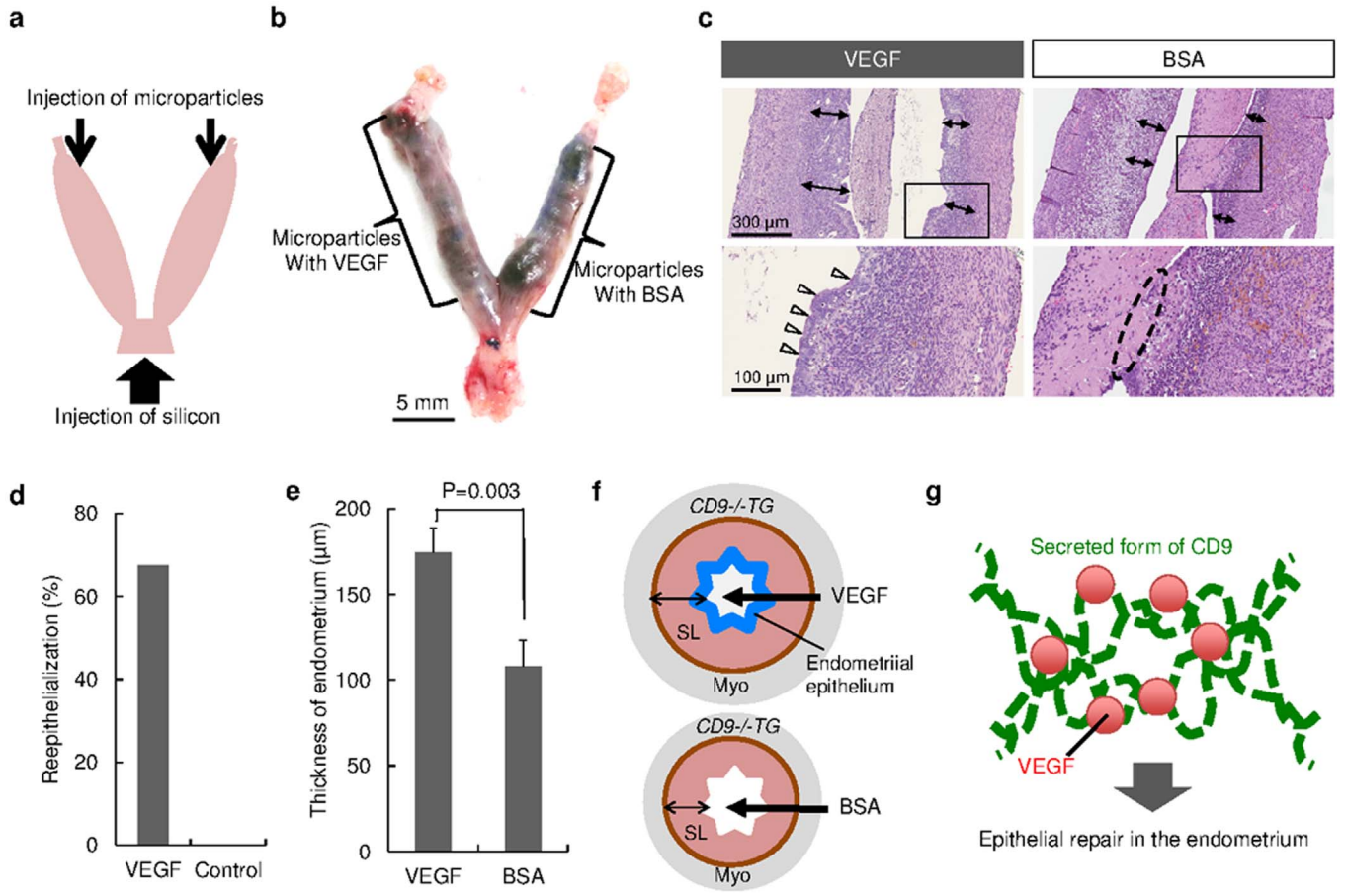

Figure 5 | Endometrial epithelium repair by VEGF treatment in *Cd9*$^{-/-}$*TG* mice. (a), Experimental schematic for treatment of the endometrial epithelium of *Cd9*$^{-/-}$*TG* mice with VEGF. (b), Ventral view of the horns of a uterus isolated from a *Cd9*$^{-/-}$*TG* mouse at 1 week after VEGF-linked microparticles were injected into the uterine cavity. Scale bar, 5 mm. (c), Endometrial epithelium treated with VEGF or BSA as a control. Lower panels, enlarged images of boxes in the upper panels. Double-headed arrows indicate the endometrial thickness. Hollow arrowheads indicate the re-epithelialized layers. The dotted circle indicates the fused site of endometrial stromal layers without epithelium with a mixture of microparticles and immune cells. Scale bars, 300 μm in upper panels and 100 μm in lower panels. (d), The rate of re-epithelialized sites in the *Cd9*$^{-/-}$*TG* endometrium treated with VEGF or BSA. (e), Thickness of the endometrium treated with VEGF or BSA. Values are the mean ± SE. (f), Schematic model of re-epithelialization of the endometrium treated with VEGF. The endometrial thickness was measured at the site indicated with double-headed arrows. SL, stromal layers; Myo, myometrium. (g), Schematic model of CD9 and VEGF secretion from epithelial cells. CD9-mediated VEGF release contributes to endometrial re-epithelialization.

Cd9$^{-/-}$ mice and unmatured oocytes of *Cd9*$^{+/+}$ mice[16]. These results indicate that a more specific mechanism controls the extracellular release of CD9, which is presumably related to the internal concentration of hormones depending on the female sexual cycle, as shown in Fig. 1d.

Because the reduction of the litter size of *Cd9*$^{-/-}$*TG* mice was not correlated with age, we considered that their endometrium was repaired during the estrous cycle, even in the absence of CD9 (Fig. 3c). In contrast, because the endometrial cavity of *Cd9*$^{-/-}$*TG* mice was narrowed, there may be a common mechanism underlying the endometrial repair, which works in both cyclic repair and repair after parturition. There are at least two possible mechanisms: (1) a mechanism regulated by MMPs and integrins as described previously[1] and (2) a mechanism regulated by CD9-mediated VEGF secretion. Both mechanisms would act in endometrial repair, but CD9-mediated VEGF secretion would contribute more to the endometrial repair after parturition than the cyclic repair.

In conclusion, we found that 1) a reduction of the amount of CD9 in uterine secretions and thinning of the endometrial thickness are correlated with the failure rate of pregnancy in patients; 2) CD9 deficiency causes reduced endometrial repair after parturition, leading to a reduction of fecundity; 3) CD9-mediated exocytosis plays a role in VEGF secretion.

Methods

Antibodies and chemicals. For immunohistochemistry and immunoblotting, a rat anti-mouse CD9 monoclonal antibody (mAb) (clone KMC8) and mouse anti-human CD9 mAb (clone ALB6) were purchased from BD Biosciences (San Jose, CA), and a mouse anti-mouse vascular endothelial growth factor (VEGF) mAb (clone RM0009-2G02) was purchased from Abcam. For immunohistochemistry, rat anti-integrin α6 and β1, and CD98 mAbs (clones GoH3, KMI6, and H202-141, respectively) were purchased from BD Biosciences, a rat anti-E-cadherin mAb (clone DECMA-1) was purchased from Sigma-Aldrich, and a rabbit anti-HIF-1α polyclonal antibody was purchased from Novus Biologicals. Secondary antibodies for immunohistochemistry were Alexa Fluor 488- and 546-conjugated IgGs purchased from Molecular Probes. Horseradish peroxidase-conjugated secondary antibodies (Sigma-Aldrich) were used for immunoblotting. Nuclei were counterstained with 4′, 6-diamidino-2-phenylindole (DAPI) (WAKO Pure Chemical Industries).

Immunoblotting of uterine secretions. Two patient groups were recruited from the outpatient department of the Fertility Clinic Tokyo (Tokyo, Japan) and St. Women's Clinic, Tokyo, Japan (Saitama, Japan). One group included 115 women with recurrent implantation failure (RIF). Patients in this group had received transfers of good quality embryos at least twice, but had not achieved pregnancy. A blastocyst with a grade higher than BB according to Gardner's criteria[47] was categorized as "good quality" in this study. The other group was a control including 56 women who had first visited the clinics with complaint of infertility within 6 months before the

following examination. This group of patients had never received embryo transfers. Patients were excluded who had uterine endometrial irregularity including endometrial polyp or submucosal myoma, amenorrhea because of premature ovarian insufficiency, or were over 43 years of age. Clinical data were analyzed by chi-square test and residual analysis. $P < 0.05$ was considered to be statistically significantly different. Informed consent was provided by all patients for this study.

Patient samples were collected at the mid luteal phase, the fifth to seventh day post-ovulation, which is considered to be an implantation window[48]. An 8-Fr Foley catheter connected to the disposable 5-ml syringe (TERUMO) was inserted into the uterine cavity through the cervix. Five milliliters of saline (Otsuka Pharmaceutical) was then injected into the cavity, immediately aspirated without contamination by the vaginal and cervical fluids, and collected in eppendorf tubes. The collected uterine flushing was centrifuged at 1500 *g* for 10 min at room temperature to remove blood corpuscles, exfoliated epithelial cells and large protein complexes. The supernatants were then transferred to new eppendorf tubes, heated for inactivation of endogenous proteases, and then stored at −20°C until use. The protein concentration of each sample was measured by the Biuret test[49]. Samples (50 μl) of human or mouse uterine secretions (as detailed below) were boiled at 95°C for 10 min in 50 μl Laemmli's SDS sample buffer containing 2% SDS, 62.5 mM Tris-HCl (pH 6.8), 0.005% bromophenol blue, and 7% glycerol. Then, 10 μl samples were resolved by SDS-polyacrylamide gel electrophoresis on 10% acrylamide gels and then transferred to Immobilon-FC (Millipore). Detection of immune complexes formed by proteins of interest and primary antibodies was performed by enzyme-linked color development with horseradish peroxidase conjugated to secondary antibodies. The intensity of the band was quantified using NIH Image J software. Briefly, the signal was outlined and the mean intensity and background fluorescence were measured. The specific signal was calculated by dividing the band intensities for CD9 by those for actin. If the relative band intensitiy for CD9 was less than 0.01, the sample was considered as "CD9 negative" in this study.

This study was approved by the Ethics Committee at the Japanese Institution for Standardizing Assisted Reproductive Technology (#11-09). Samples were collected only from patients who had provided informed consent.

Animals. Eight- to 12-week-old female C57BL/6N mice and male B6C3F1 mice, a cross between female C57BL/6N and male C3H mice, were purchased from SLC (Shizuoka, Japan).

Cd9$^{-/-}$ mice were generated as described previously[13], and backcrossed with a C57BL/6N genetic background. *Cd9*$^{-/-}$ mice expressing CD9 tagged at the N-terminus with GFP (CD9-GFP) (*Cd9*$^{-/-}$*TG*) were generated as described previously[16]. The construct carrying mouse CD9 tagged at the C-terminus with GFP (CD9-GFP) was sub-cloned into plasmid DNA containing the mouse ZP3 promoter[50]. Transgenic mice with a *Cd9*$^{-/-}$ background were produced by crossmating with *Cd9*$^{-/-}$ mice. The genotypes of mice were determined by standard procedures as described previously[16].

All mice were housed under specific pathogen-free controlled conditions. Food and water were available *ad libitum*. The procedures for performing animal experiments were in accordance with the principles and guidelines of the Care and Use of Laboratory Animals at the National Research Institute for Child Health and Development. The animal committee of the National Research Institute for Child Health and Development approved the experiments including the use of live animals (Experimental number is 04-004).

Vaginal smear test and collection of mouse uterine secretions. *Cd9*$^{-/-}$*TG* and *Cd9*$^{+/+}$ female mice were examined by vaginal smear cytology and assigned to one of four phases of the estrous cycle as described previously[4] (Supplementary Fig. 1a). Briefly, a vaginal smear was collected with a moistened cotton swab, applied to a glass slide, stained with hematoxylin, and then observed under a stereomicroscope. According to the microscopic characteristics of the vaginal smear, the mice were classified as proestrus, estrus, metestrus, or diestrus. Because the uterus undergoes hormonal changes during the estrous cycle, and is distended at the estrus stage because of an increase of uterine secretions, we collected the uterine secretions from estrus-stage mice. Mice staged at estrus were sacrificed and their uteri were incised and flushed with 50 μl saline. Then, the flushed solution was collected from each of uterine horns and subjected to immunoblotting as described above.

Immunohistochemical analysis of mouse uterine tissues. Estrus-stage female mice were sacrificed and their uteri were excised and fixed with 4% paraformaldehyde for 3 h at 4°C. After fixation, the uterine tissues were immersed in a 30% sucrose solution at 4°C until they sank to the bottom of the tubes and then embedded in OCT (Tissue-Tek) and frozen at −80°C. The tissues were then sectioned at 10 μm with a cryostat (CryoStar NX70; Thermo Scientific). The sections were dried and incubated with primary antibodies (2.5 μg/ml) in HEPES-buffered saline (HBS; 10 mM HEPES (pH 8.0), 0.15 M NaCl, and 3% fetal bovine serum [FBS]) for 2 h at room temperature, and then Alexa Fluor 488- or 546-conjugated IgGs, followed by three washes in HBS. Nuclei were then counterstained with DAPI at a final concentration of 10 μg/ml in HBS for 30 min at room temperature, followed by three washes in HBS. Images were captured under a laser scanning confocal microscope (LSM 510 model; Carl Zeiss Microimaging, Thornwood, NY).

Wound healing assay. For the wound healing assay, three uteri each were harvested from sacrificed *Cd9*$^{-/-}$*TG* and *Cd9*$^{+/+}$ mice, and the endometrial epithelial cells were isolated by treatment with collagenase (WAKO Pure Chemical Industries) as described previously[51]. Briefly, uterine inner surfaces were treated with collagenase for 1 h at 37°C, and the uterine fluid was collected from intrauterine cavities. Then, the endometrial epithelial cells were centrifuged at 1,000 rpm for 10 min, washed with complete medium (Dulbecco's modified Eagles medium containing 20% FBS, 0.1 mg/ml heparin, 0.1 mg/ml endothelial cell mitogen [Biomedical Technologies], nonessential amino acids, sodium pyruvate, L-glutamine, and penicillin/streptomycin at standard concentrations), and cultured in fibronectin-coated tissue culture dishes (Asahi glass). Non-adherent cells were removed by changing the medium after 24 h.

After serum starvation, the confluent monolayer of epithelial cells was wounded lengthwise with a 200-μl pipette tip. Phase contrast images of the wounds were taken at 0, 3.5, and 17.5 h after the epithelial cells were injured at three random locations to examine the extent of wound closure using ImageJ software (National Institutes of Health, USA).

Immuno-electron microscopic analysis. Uterine secretions collected from *Cd9*$^{-/-}$*TG* and *Cd9*$^{+/+}$ female mice were incubated with an anti-CD9 mAb (0.5 μg/ml) at room temperature for 2 h and then 10 nm colloidal gold particles coupled to secondary antibodies at room temperature for 1 h. The samples were centrifuged at 12,000 rpm for 30 min at room temperature, and then the precipitates were washed three times with HBS. The precipitates were then fixed with glutaraldehyde and osmic acid solutions. Ultrathin sections were prepared as described previously[52].

Multiplex suspension array. Multiplex bead kits were purchased from the following manufacturers: LINCO Research (Kit a), Bio-Rad Laboratories (Kit b), R&D Systems (Kit c), and BioSource International (Kit d). The multiplex assay was performed to detect cytokines of interest in sextaplicate on two separate occasions according to the manufacturers' instructions. Standard curves for each cytokine using each kit were generated using the reference cytokine concentrations supplied by the manufacturers. Raw data (mean fluorescence intensity) from all kits were analyzed by MasterPlex Quantitation Software (MiraiBio) to obtain concentration values.

Repair of the endometrial epithelium by treatment with VEGF. To repair the endometrial epithelium damaged by parturition, VEGF was injected into the uterine cavity of *Cd9*$^{-/-}$*TG* female mice. To sustain the effect of VEGF in the uterine cavity, VEGF was covalently coupled to carboxylated microparticles (6 μm average diameter) (Polyscience). Briefly, 12.5 mg microparticles was suspended in 0.17 ml PolyLink Coupling Buffer containing 50 mM 2-(N-morpholino)ethanesulfonic acid (pH 5.2) and 0.05% Proclin-300. Twenty microliters of 200 mg/ml 1-ethyl-3-(3-dimethylaminopropyl)carbodiimide was added to the microparticle suspension. After gentle mixing, the microparticles were combined with 200 μg recombinant mouse VEGF (164 amino acid; R&D Systems) and incubated for 1 h at room temperature. After centrifugation for 10 min at 500 *g*, the microparticles were resuspended in 0.4 ml PolyLink Wash/Storage Buffer containing 10 mM Tris-HCl (pH 8.0), 0.05% bovine serum albumin (BSA), and 0.05% Proclin-300, and then stored at 4°C. Before VEGF injection, *Cd9*$^{-/-}$*TG* female mice were intercrossed with *Cd9*$^{-/-}$ male mice to deliver pups. At 1 week after parturition, mother mice were anesthetized with Avertin and their vaginas were filled with silicon using a 1-ml syringe attached to a 200-μl pipette tip, and the uterus was filled with VEGF-linked microparticles from backside lesions. Silicon (BECKMAN COULTER) was used to prevent VEGF-linked microparticles from leaking into the vagina and contaminating with BSA-linked microparticles in another uterine horn. At 7 days after microparticle injection, the mice were sacrificed and their uteri were examined histochemically by hematoxylin and eosin (H&E) staining. The rate of the repithelialization was calculated by (number of repithelialized site)/(total number of implantation site).

Statistical analysis. Comparisons were made using one-way analysis of variance following Scheffe's method, the Mann-Whitney U-test, or Fisher's exact test. Statistical significance was defined as $P < 0.05$. Results were expressed as the mean ± SEM.

1. Salamonsen, L. A. Tissue injury and repair in the female human reproductive tract. *Reproduction* **125**, 301–311 (2003).
2. Hawkins, S. M. & Matzuk, M. M. The menstrual cycle: basic biology. *Ann N Y Acad Sci* **1135**, 10–18 (2008).
3. Cross, J. C., Werb, Z. & Fisher, S. J. Implantation and the placenta: key pieces of the development puzzle. *Science* **266**, 1508–1518 (1994).
4. Caligioni, C. S. Assessing reproductive status/stages in mice. *Curr Protoc Neurosci* **Appendix 4**, Appendix 4I (2009).
5. Hemler, M. E. Targeting of tetraspanin proteins--potential benefits and strategies. *Nat Rev Drug Discov* **7**, 747–758 (2008).
6. Miyake, M., Koyama, M., Seno, M. & Ikeyama, S. Identification of the motility-related protein (MRP-1), recognized by monoclonal antibody M31-15, which inhibits cell motility. *J Exp Med* **174**, 1347–1354 (1991).
7. Wynne, F. *et al.* Mouse pregnancy-specific glycoproteins: tissue-specific expression and evidence of association with maternal vasculature. *Reproduction* **131**, 721–732 (2006).
8. Denzer, K., Kleijmeer, M. J., Heijnen, H. F., Stoorvogel, W. & Geuze, H. J. Exosome: from internal vesicle of the multivesicular body to intercellular signaling device. *J Cell Sci* **113 Pt 19**, 3365–3374 (2000).

9. Wubbolts, R. *et al.* Proteomic and biochemical analyses of human B cell-derived exosomes. Potential implications for their function and multivesicular body formation. *J Biol Chem* **278**, 10963–10972 (2003).
10. Caby, M. P., Lankar, D., Vincendeau-Scherrer, C., Raposo, G. & Bonnerot, C. Exosomal-like vesicles are present in human blood plasma. *Int Immunol* **17**, 879–887 (2005).
11. Valadi, H. *et al.* Exosome-mediated transfer of mRNAs and microRNAs is a novel mechanism of genetic exchange between cells. *Nat Cell Biol* **9**, 654–659 (2007).
12. Thery, C. *et al.* Molecular characterization of dendritic cell-derived exosomes. Selective accumulation of the heat shock protein hsc73. *J Cell Biol* **147**, 599–610 (1999).
13. Miyado, K. *et al.* Requirement of CD9 on the egg plasma membrane for fertilization. *Science* **287**, 321–324 (2000).
14. Le Naour, F., Rubinstein, E., Jasmin, C., Prenant, M. & Boucheix, C. Severely reduced female fertility in CD9-deficient mice. *Science* **287**, 319–321 (2000).
15. Kaji, K. *et al.* The gamete fusion process is defective in eggs of Cd9-deficient mice. *Nat Genet* **24**, 279–282 (2000).
16. Miyado, K. *et al.* The fusing ability of sperm is bestowed by CD9-containing vesicles released from eggs in mice. *Proc Natl Acad Sci U S A* **105**, 12921–12926 (2008).
17. Devaux, P. F. Protein involvement in transmembrane lipid asymmetry. *Annu Rev Biophys Biomol Struct* **21**, 417–439 (1992).
18. Park, K. R. *et al.* CD9 is expressed on human endometrial epithelial cells in association with integrins alpha(6), alpha(3) and beta(1). *Mol Hum Reprod* **6**, 252–257 (2000).
19. Hasuwa, H. *et al.* CD9 amino acids critical for upregulation of diphtheria toxin binding. *Biochem Biophys Res Commun* **289**, 782–790 (2001).
20. Dominguez, F. *et al.* Human endometrial CD98 is essential for blastocyst adhesion. *PLoS One* **5**, e13380 (2010).
21. Singh, H. & Aplin, J. D. Adhesion molecules in endometrial epithelium: tissue integrity and embryo implantation. *J Anat* **215**, 3–13 (2009).
22. Feral, C. C. *et al.* CD98hc (SLC3A2) participates in fibronectin matrix assembly by mediating integrin signaling. *J Cell Biol* **178**, 701–711 (2007).
23. Spits, H. & Di Santo, J. P. The expanding family of innate lymphoid cells: regulators and effectors of immunity and tissue remodeling. *Nat Immunol* **12**, 21–27 (2011).
24. Dimitriadis, E., White, C. A., Jones, R. L. & Salamonsen, L. A. Cytokines, chemokines and growth factors in endometrium related to implantation. *Hum Reprod Update* **11**, 613–630 (2005).
25. Rossi, M. *et al.* Identification of genes regulated by interleukin-1beta in human endometrial stromal cells. *Reproduction* **130**, 721–729 (2005).
26. Makkar, G., Ng, E. H., Yeung, W. S. & Ho, P. C. Excessive ovarian response is associated with increased expression of interleukin-2 in the periimplantation endometrium. *Fertil Steril* **91**, 1145–1151 (2009).
27. Fishman, P. *et al.* Prevention of fetal loss in experimental antiphospholipid syndrome by in vivo administration of recombinant interleukin-3. *J Clin Invest* **91**, 1834–1837 (1993).
28. Katano, K. *et al.* Low serum M-CSF levels are associated with unexplained recurrent abortion. *Am J Reprod Immunol* **38**, 1–5 (1997).
29. Ashkar, A. A., Di Santo, J. P. & Croy, B. A. Interferon gamma contributes to initiation of uterine vascular modification, decidual integrity, and uterine natural killer cell maturation during normal murine pregnancy. *J Exp Med* **192**, 259–270 (2000).
30. Stordeur, P. & Goldman, M. Interleukin-10 as a regulatory cytokine induced by cellular stress: molecular aspects. *Int Rev Immunol* **16**, 501–522 (1998).
31. Seder, R. A., Gazzinelli, R., Sher, A. & Paul, W. E. Interleukin 12 acts directly on CD4+ T cells to enhance priming for interferon gamma production and diminishes interleukin 4 inhibition of such priming. *Proc Natl Acad Sci U S A* **90**, 10188–10192 (1993).
32. Kaitu'u-Lino, T. J., Morison, N. B. & Salamonsen, L. A. Neutrophil depletion retards endometrial repair in a mouse model. *Cell Tissue Res* **328**, 197–206 (2007).
33. Semerad, C. L., Liu, F., Gregory, A. D., Stumpf, K. & Link, D. C. G-CSF is an essential regulator of neutrophil trafficking from the bone marrow to the blood. *Immunity* **17**, 413–423 (2002).
34. Chou, R. C. *et al.* Lipid-cytokine-chemokine cascade drives neutrophil recruitment in a murine model of inflammatory arthritis. *Immunity* **33**, 266–278 (2010).
35. Moser, B., Wolf, M., Walz, A. & Loetscher, P. Chemokines: multiple levels of leukocyte migration control. *Trends Immunol* **25**, 75–84 (2004).
36. Ferrara, N., Gerber, H. P. & LeCouter, J. The biology of VEGF and its receptors. *Nat Med* **9**, 669–676 (2003).
37. Kim, M. *et al.* VEGF-A regulated by progesterone governs uterine angiogenesis and vascular remodelling during pregnancy. *EMBO Mol Med* (2013).
38. Boesen, T. P., Soni, B., Schwartz, T. W. & Halkier, T. Single-chain vascular endothelial growth factor variant with antagonist activity. *J Biol Chem* **277**, 40335–40341 (2002).
39. Nothnick, W. B., Soloway, P. & Curry, T. E., Jr. Assessment of the role of tissue inhibitor of metalloproteinase-1 (TIMP-1) during the periovulatory period in female mice lacking a functional TIMP-1 gene. *Biol Reprod* **56**, 1181–1188 (1997).
40. Marzesco, A. M. *et al.* Release of extracellular membrane vesicles from microvilli of epithelial cells is enhanced by depleting membrane cholesterol. *FEBS Lett* **583**, 897–902 (2009).
41. Fan, X. *et al.* VEGF blockade inhibits angiogenesis and reepithelialization of endometrium. *FASEB J* **22**, 3571–3580 (2008).
42. Ng, Y. H. *et al.* Endometrial exosomes/microvesicles in the uterine microenvironment: a new paradigm for embryo-endometrial cross talk at implantation. *PLoS One* **8**, e58502 (2013).
43. Komada, Y. *et al.* Shedding of CD9 antigen into cerebrospinal fluid by acute lymphoblastic leukemia cells. *Blood* **76**, 112–116 (1990).
44. Epple, L. M. *et al.* Medulloblastoma exosome proteomics yield functional roles for extracellular vesicles. *PLoS One* **7**, e42064 (2012).
45. Blackman, M. R. *et al.* Human placental and pituitary glycoprotein hormones and their subunits as tumor markers: a quantitative assessment. *J Natl Cancer Inst* **65**, 81–93 (1980).
46. Baker, R. M., Hirschberg, C. B., O'Brien, W. A., Awerbuch, T. E. & Watson, D. Isolation of somatic cell glycoprotein mutants. *Methods Enzymol* **83**, 444–458 (1982).
47. Teranishi, A., Kuwata, A., Fumino, T., Hamai, H. & Shigeta, M. A theoretical model for single blastocyst transfer. *J Assist Reprod Genet* **26**, 327–334 (2009).
48. Paria, B. C., Huet-Hudson, Y. M. & Dey, S. K. Blastocyst's state of activity determines the "window" of implantation in the receptive mouse uterus. *Proc Natl Acad Sci U S A* **90**, 10159–10162 (1993).
49. Tamm, I. & Horsfall, F. L., Jr. Characterization and separation of an inhibitor of viral hemagglutination present in urine. *Proc Soc Exp Biol Med* **74**, 106–108 (1950).
50. Rankin, T. L. *et al.* Human ZP3 restores fertility in Zp3 null mice without affecting order-specific sperm binding. *Development* **125**, 2415–2424 (1998).
51. Fernandez-Shaw, S., Shorter, S. C., Naish, C. E., Barlow, D. H. & Starkey, P. M. Isolation and purification of human endometrial stromal and glandular cells using immunomagnetic microspheres. *Hum Reprod* **7**, 156–161 (1992).
52. Toshimori, K., Saxena, D. K., Tanii, I. & Yoshinaga, K. An MN9 antigenic molecule, equatorin, is required for successful sperm-oocyte fusion in mice. *Biol Reprod* **59**, 22–29 (1998).

Acknowledgments

This study was supported by a grant from The Ministry of Health, Labour and Welfare, and a Grant-in-aid for Scientific Research from The Ministry of Education, Culture, Sports, and Technology of Japan.

Author contributions

K.M. and T.H. conceived and designed the experiments. N.K., N.Y. and S.K. performed the experiments. K.M., T.H., N.K., H.S., M.M., N.I., Y.O. and A.U. analyzed the data. K.M., T.H. and N.K. wrote the manuscript and prepared figures. All authors reviewed the manuscript.

Additional information

Supplementary information accompanies this paper at http://www.nature.com/scientificreports

Competing financial interests: The authors declare no competing financial interests.

How to cite this article: Kawano, N. *et al.* Absence of CD9 reduces endometrial VEGF secretion and impairs uterine repair after parturition. *Sci. Rep.* **4**, 4701; DOI:10.1038/srep04701 (2014).